

# Space-variant processing of 1-D signals

Robert J. Marks II, John F. Walkup, Marion O. Hagler, and Thomas F. Krile

Two general schemes for 1-D space-variant processing are proposed. The direct output display scheme gives the space-variant system output along a line in the processor's output plane. The output spectrum display scheme directly computes the space-variant system's output spectrum. Both of these schemes utilize a 1-D input and a line spread function mask. Example applications and experimental results are also presented.

## I. Introduction

Coherent optical processors, although traditionally used to execute space-invariant computations, are in many cases capable of accomplishing space-variant operations. These include coordinate distortion,<sup>1-5</sup> integral transform evaluation,<sup>6-8</sup> and ambiguity function display.<sup>9-11</sup> Space-variant analysis has also proven useful in such areas as image restoration<sup>12,13</sup> and handwriting synthesis.<sup>14</sup> Schemes have been proposed whereby arbitrary 2-D space-variant systems may be represented with the use of a volume hologram.<sup>15-18</sup> A review of the various methods of space-variant processing is given by Goodman.<sup>19</sup>

The potential utilization of the parallel processing of coherent systems to perform general 1-D space-variant operations was recognized by Cutrona *et al.*<sup>20,21</sup> Specifically, he proposed a coherent system for performing the general linear operation

$$\int_{-\infty}^{\infty} k(x;\xi)f(\xi)d\xi,$$

where  $k(x;\xi)$  is the kernel of the linear operator, and  $f(\xi)$  is an input function. Advances in areas of coherent processing since this suggestion, including computer generated holograms and electrical-to-optical transducers, make the 1-D approach to coherent space-variant processing rather easily implementable. The further capability of performing real time processing of temporal signals makes such a scheme potentially powerful.

It is our purpose here to present two rather general techniques for 1-D space-variant processing. Both employ a 1-D input placed adjacent to a transparency whose transmittance represents the system line spread

function. Spherical or cylindrical lenses are utilized to perform appropriate Fourier transformation and imaging. The desired system output is viewed along a line in an output plane.

The first of the two schemes to be discussed we will call the direct output display (DOD) method. Specific space-variant operations, which may be accomplished with the DOD processor include magnification, coordinate distortion, real time convolution and correlation, integral transform evaluation, and ambiguity function display.

The second scheme, called the output spectrum display (OSD) method, directly computes the Fourier transform of the space-variant system output. This processor employs a single spherical lens. The 1-D output spectrum appears along a 45° line in the processor's output plane. Specific applications include cross spectral density function display and spectral magnification.

Other areas addressed in this paper include lensless space-variant processing where required lens transmittances are included on the line spread function mask. Geometric interpretations of the function shifts encountered in 1-D convolution and correlation are discussed. Experimental results are also presented.

## II. Preliminaries

The output  $g(x)$  of a linear system due to an input  $f(\xi)$  may be determined by the superposition integral<sup>22</sup>:

$$\begin{aligned} g(x) &= S[f(\xi)] \\ &= \int_{-\infty}^{\infty} f(\xi)h(x - \xi;\xi)d\xi, \end{aligned} \quad (1)$$

where  $S[\cdot]$  is the linear system operator. The system line spread function is the system's response to an input Dirac delta:

$$h(x - \xi;\xi) = S[\delta(x - \xi)]. \quad (2)$$

As will be made clear in the development to follow, this

T. F. Krile is with Rose-Hulman Institute of Technology, Department of Electrical Engineering, Terre Haute, Indiana 47801; the other authors are with Texas Tech University, Department of Electrical Engineering, Lubbock, Texas 79409.

Received 2 September 1976.

particular line spread function notation has certain advantages in characterizing space-variant systems.<sup>23</sup>

We say that a system is space-invariant (or isoplanatic) if the line spread function shifts directly with the input and is thus a function of only  $(x - \xi)$ :

$$h(x - \xi; \xi) \rightarrow h(x - \xi). \quad (3)$$

If a linear system does not meet the invariance criterion of Eq. (3), we say that it is space-variant.

It is the superposition integral characterization of space-variant systems [Eq. (1)] or various forms thereof, which we are interested in evaluating by optical means. Coherent processors capable of performing such 1-D operations are presented in the sections to follow.

### III. Direct Output Display Method

A coherent processor capable of evaluating the superposition integral<sup>21</sup> is pictured in Fig. 1. The 1-D input  $f(\xi)$  is placed in plane  $P_1$  directly adjacent to a mask on which the system line spread function  $h(x - \xi; \xi)$  is recorded. Note that  $f(\xi)$  covers the entire  $(x, \xi)$  plane with no variation in the  $x$  direction. Cylindrical lenses  $L_1$ ,  $L_2$ , and  $L_3$  have respective focal lengths of

$$2f_1 = f_2 = 2f_3. \quad (4)$$

As such, Fourier transformation is performed in the  $\xi$  direction, and imaging is performed in the  $x$  direction. The field amplitude  $g_0(x, \nu)$  on the output plane  $P_2$  is then given by

$$g_0(x, \nu) = \int_{-\infty}^{\infty} f(\xi) h(x - \xi; \xi) \exp(-j2\pi\nu\xi) d\xi, \quad (5)$$

where the spatial frequency  $\nu$  is related to the actual horizontal distance  $x_2$  on plane  $P_2$  by

$$\nu = x_2/\lambda f_2. \quad (6)$$

Here,  $\lambda$  is the wavelength of the spatially coherent illumination.

Comparing the superposition integral in Eq. (1) with the processor output [Eq. (5)], we find that

$$g(x) = g_0(x, 0). \quad (7)$$

That is, the 1-D output, corresponding to the input and line spread function mask, appears in the processor output plane along the  $x$  axis. The desired space-variant operation has thus been performed. For later reference, this processing scheme, or modifications thereof, will be referred to as the direct output display or DOD method.

An alternate and somewhat simpler scheme for performing 1-D Fourier transformation<sup>5</sup> is pictured in Fig. 2. As shown, spherical and cylindrical lenses, placed back to back, replace the three cylindrical lenses in Fig. 1. If we assign a focal length of  $f$  to both the spherical and cylindrical lens, this processor's output intensity distribution is the same as in Fig. 1 with  $\nu = x_2/\lambda f$ .

With the concept of the DOD processor firmly established, we shall now present some specific applications.

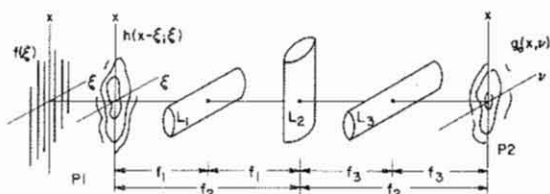


Fig. 1. A coherent optical processor for performing 1-D space-variant operations. The desired processor output lies along the  $x$  axis on plane  $P_2$ .

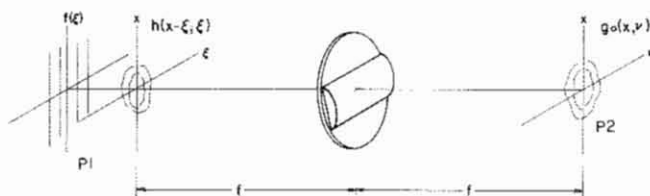


Fig. 2. Another coherent processor for performing 1-D space-variant operations. The intensity distribution on  $P_2$  is identical to that in Fig. 1.

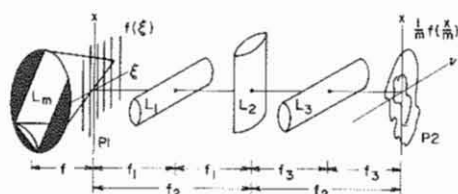


Fig. 3. DOD processor for performing 1-D magnification. The magnification is equal to the slope of lens  $L_m$  which is mounted on a rotatable assembly.

#### A. One-Dimensional Magnification

The ideal magnifier is characterized by the input-output relationship

$$g(x) = \frac{1}{M} f(x/M), \quad (8)$$

where  $M$  is the magnification. The corresponding line spread function is

$$h(x - \xi; \xi) = \delta(x - M\xi). \quad (9)$$

On the  $(x, \xi)$  plane, we interpret this relation as a Dirac delta sheet along the line  $x = M\xi$ . The magnification is simply the line's slope.

We may implement the DOD magnifier as shown in Fig. 3. The Dirac delta sheet is formed by focusing a plane wave with a cylindrical lens mounted on a rotatable assembly. (This configuration replaces the previously employed line spread function mask.) We may change the slope of this sheet, and thus the resulting magnification, by simply rotating the lens.

At the lens's back focal plane we place the input  $f(\xi)$ . As before, Fourier transformation is performed in the  $\xi$  direction by cylindrical lenses  $L_1$ ,  $L_2$ , and  $L_3$ . The desired output,  $(1/M) f(x/M)$ , appears on plane  $P_2$  along the  $x$  axis. For the case of a double pulse input,

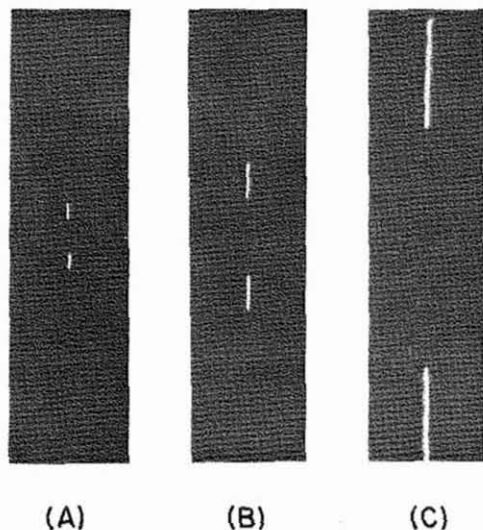


Fig. 4. The output of the DOD processor in Fig. 3 to a double square pulse input. The magnifications are (a)  $M = \frac{1}{2}$ , (b)  $M = 1$ , (c)  $M = 3$ .

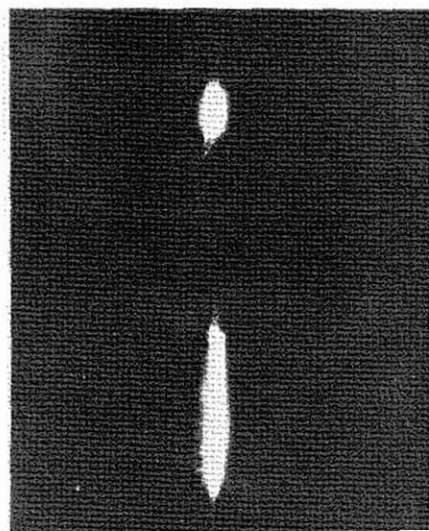


Fig. 5. Output of a piecewise magnifier distortion processor corresponding to the inputs pictured in Fig. 6. The larger pulse is roughly three times the length of the smaller.

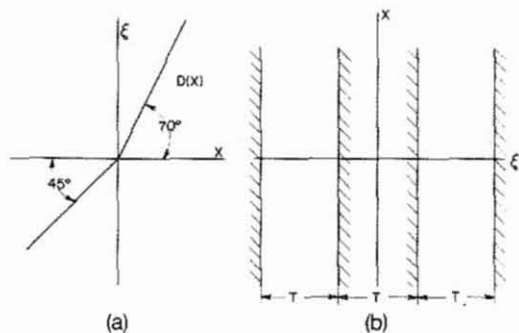


Fig. 6. Inputs for piecewise magnification coordinate distortion DOD processor: (a) The distortion function  $D(x)$ . For  $\xi > 0$ , we have magnification of  $\tan 70^\circ \approx 3$ . For  $\xi < 0$ ,  $\tan 45^\circ = 1$ . (b) Double square pulse input.

experimental results using this setup are shown in Fig. 4 for various values of  $M$ . Note that, although 2-D magnification is optically trivial, no conventional scheme can control the magnification parameter from a single plane as it is done here.

### B. Coordinate Distortion

The magnifier scheme may be generalized to linear systems with input-output relationships of the form

$$g(x) = f[D(x)], \quad (10)$$

where we shall refer to  $D(x)$  as the distortion function. The line-spread function associated with Eq. (10) is

$$h(x - \xi; \xi) = \delta[\xi - D(x)]. \quad (11)$$

Our Dirac delta sheet is now bent along the locus  $\xi = D(x)$  on the  $(x, \xi)$  plane. Such a bent Dirac delta may be crudely generated by an appropriately bent glass rod which acts as a curved cylindrical lens. Experimental results, using a glass rod with a single bend, are shown in Fig. 5. The resulting lens slopes, as shown in Fig. 6(a), constitute different magnifications for  $\xi > 0$  and  $\xi < 0$ . The DOD processor output, for the input pulse configuration in Fig. 6(b), is shown in Fig. 5.

An alternate form of distortion, used by Rhodes,<sup>3</sup> employs the line spread function

$$h(x - \xi; \xi) = \exp[-j2\pi\xi D(x)]. \quad (12)$$

Here, the system output is a distorted version of the input's spectrum

$$\begin{aligned} g(x) &= \int_{-\infty}^{\infty} f(\xi) \exp[-j2\pi\xi D(x)] d\xi \\ &= F[D(x)], \end{aligned} \quad (13)$$

where  $F(\nu)$  is the Fourier transform of the input

$$F(\nu) = \int_{-\infty}^{\infty} f(\xi) \exp(-j2\pi\nu\xi) d\xi. \quad (14)$$

Rhodes<sup>3</sup> uses such a system for generating a log-frequency display of the input by utilizing a distortion function proportional to  $\ln x$ .

### C. Real Time Convolution and Correlation

The capability of conventional coherent processors to perform 2-D convolution is well known. All these schemes, however, either necessitate encoding the Fourier transform of a function on a transparency or require motion. As we will show, 1-D convolution may be performed with a variation of the DOD processor with no requirement of motion or Fourier encoding.

The convolution integral, descriptive of isoplanatic systems, is obtained by substituting the invariance criterion of Eq. (3) into the superposition integral [Eq. (1)]:

$$\begin{aligned} g(x) &= \int_{-\infty}^{\infty} f(\xi) h(x - \xi) d\xi \\ &= f(x) * h(x), \end{aligned} \quad (15)$$

where  $*$  denotes convolution. The similar operation of correlation is defined as

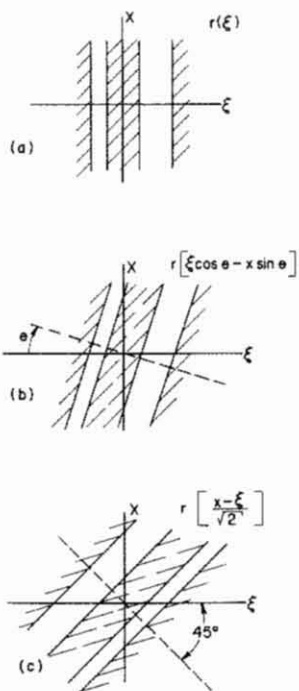


Fig. 7. (a) A 1-D function  $r(\xi)$  on the  $(x, \xi)$  plane. (b) The transmittance in (a) rotated clockwise about the origin an angle of  $\theta$ . (c) The transmittance in (b) for  $\theta = 45^\circ$  with a coordinate reversal formed by physically rotating (b) about its  $\xi$  and  $x$  axes.

$$g(x) = \int_{-\infty}^{\infty} f(\xi) \bar{s}(\xi - x) d\xi = f(x) \star s(x), \quad (16)$$

where the underbar denotes complex conjugate and  $\star$  denotes correlation.

Before presenting the DOD processors capable of performing convolution and correlation, we digress briefly for a discussion of the geometrical interpretations of the spatial shifts encountered in both Eqs. (15) and (16). Consider the 1-D function  $r(\xi)$  on the  $(x, \xi)$  plane as pictured in Fig. 7(a). If we rotate this transparency about the origin through an angle of  $\theta$  in the clockwise sense [Fig. 7(b)], the resulting 2-D function is described by

$$r(\xi \cos \theta - x \sin \theta). \quad (17)$$

For the case of a  $45^\circ$  rotation, we obtain  $r[(\xi - x)/(2)^{1/2}]$ , which is a scaled version of the shift required by the correlation integral [Eq. (16)]. Scaling may be trivially accomplished by a conventional (2-D) imaging system with magnification  $M = 1/(2)^{1/2}$ .

Next, consider physically rotating the transparency in Fig. 7(b)  $180^\circ$  about both its  $x$  and  $\xi$  axes. This constitutes coordinate reversal. For the case of  $\theta = 45^\circ$ , the result would be the transmittance  $r[(x - \xi)/(2)^{1/2}]$ , which is the scaled shift required by the convolution integral [Eq. (15)]. Various other rotations could of course be employed to obtain a number of such shifts and scalings.

Consider, then, the DOD convolution processor as pictured in Fig. 8. In plane  $P_1$ , we place the transpar-

ency representing  $h(\xi)$  with the  $45^\circ$  rotation shown. This function,  $h[(\xi - x)/(2)^{1/2}]$  is scaled and inverted by lenses  $L_a$  and  $L_b$  which have respective focal lengths of

$$f_a = (2)^{1/2} f_b. \quad (18)$$

Incident on plane  $P_2$  is the desired  $h(x - \xi)$  which multiplies the input transmittance  $f(\xi)$ . The product is then processed as before by the three cylindrical lenses. The output  $(f \star h)$  appears along the  $x$  axis in plane  $P_3$ .

An alternate approach, not necessitating the use of the scaling lenses, will be illustrated for the case of correlation. The 1-D transmittances  $f(\xi)$  and  $s(\xi)$  are appropriately rotated  $45^\circ$  in plane  $P_1$  in Fig. 1 in such a manner to form the product

$$f \left[ \frac{(\xi + x)}{(2)^{1/2}} \right] s \left[ \frac{(\xi - x)}{(2)^{1/2}} \right]. \quad (19)$$

The field amplitude in plane  $P_2$ , after the 1-D Fourier transformation [Eq. (5)], is

$$g_0(x, \nu) = \int_{-\infty}^{\infty} f \left[ \frac{(\xi + x)}{(2)^{1/2}} \right] s \left[ \frac{(\xi - x)}{(2)^{1/2}} \right] \exp(-j2\pi\nu\xi) d\xi = (2)^{1/2} \exp(j2\pi\nu x) \int_{-\infty}^{\infty} f(\xi') s[\xi' - (2)^{1/2}x] \exp[-j2\pi[(2)^{1/2}\nu]\xi'] d\xi', \quad (20)$$

where we have made the variable substitution  $\xi' = (\xi + x)/(2)^{1/2}$ . Along the  $x$  axis, we obtain the output

$$g(x) = g_0(x, 0) = (2)^{1/2} \int_{-\infty}^{\infty} f(\xi') s[\xi' - (2)^{1/2}x] d\xi'. \quad (21)$$

This relationship is recognized as a scaled version of the correlation integral [Eq. (16)] and is thus the desired result. Convolution can of course be performed in a similar manner by choosing appropriate orientations of the 1-D input transparencies.

#### D. Entire Output Plane Utilization

There do exist some computational manipulations for which the entire output plane of the DOD processor may be utilized. Upon setting

$$h(x - \xi; \xi) = \exp(-\alpha\xi)\mu(\xi), \quad (22)$$

where  $\mu(\xi)$  is the unit step function, the DOD processor output in Eq. (5) becomes

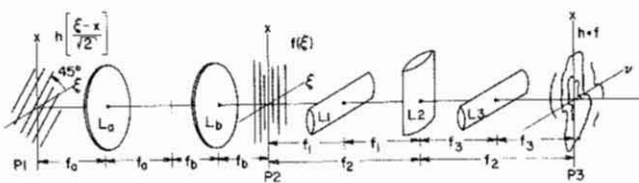


Fig. 8. DOD processor for performing convolution. Lenses  $L_a$  and  $L_b$  have focal lengths related by  $f_a = (2)^{1/2} f_b$  to perform scaling on the rotated transmittance on plane  $P_1$ .

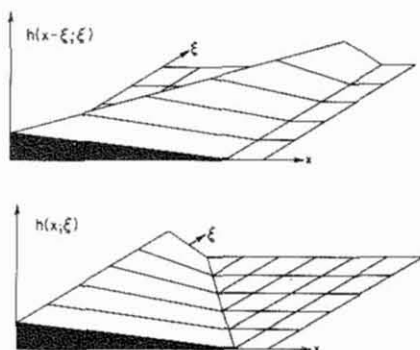


Fig. 9. An example of the relationship between the line spread function forms  $h(x - \xi; \xi)$  and  $h(x; \xi)$  on the  $(x, \xi)$  plane.

$$g_0(\alpha, \beta) = \int_0^{\infty} f(\xi) \exp[-(\alpha + j\beta)\xi] d\xi, \quad (23)$$

where

$$\beta = 2\pi\nu. \quad (24)$$

Equation (23) is immediately recognized as the one-sided Laplace transform of  $f(\xi)$  with frequency variable

$$s = \alpha + j\beta. \quad (25)$$

For this case, the  $(\alpha, \beta)$  output plane of the DOD processor may be interpreted as the complex  $s$  plane encountered in Laplace transform theory. A discussion of this specific DOD processor is given by Mueller and Carlson.<sup>6</sup>

The computation of a signal's ambiguity function is another case where the entire output plane of the DOD processor is utilized. Here, we set

$$h(x - \xi; \xi) = f(\xi - x) \quad (26)$$

so that Eq. (5) becomes the ambiguity function of the signal  $f(x)$ :

$$\chi(\nu, x) = \int_{-\infty}^{\infty} f(\xi) f(\xi - x) \exp(-j2\pi\nu\xi) d\xi. \quad (27)$$

The function  $f(\xi - x)$  may be generated by the previously discussed 45° rotation and scaling. A discussion of this particular DOD processor, with experimental results, is given by Marks *et al.*<sup>11</sup>

#### E. Integral Transform Display

We have seen that the Laplace transform of a function can be evaluated by the DOD processor. All integral transforms are, in fact, special cases of the superposition integral and thus, in principle, may be evaluated by a DOD processor. Included are the Hankel, Abel, Z, Mellin, and Fresnel transforms. Use of the Mellin transform, for example, has been proposed as an alternate to the Fourier transform for matched filtering.<sup>7</sup> We are of course limited to 1-D so that multidimensional manipulations, such as the Radon transform,<sup>24</sup> cannot be evaluated. Some transforms, such as the Hilbert, are space-invariant in nature<sup>25</sup> and may thus be evaluated by more conventional means.

#### IV. Output Spectrum Display

The direct output display or DOD method may be used to compute directly the output of a 1-D linear space-variant system. An alternate scheme, which we shall call the output spectrum display or OSD method, directly computes the Fourier transform (or spectrum) of the system output given by

$$\begin{aligned} G(f_x) &= \mathcal{F}_x[g(x)] \\ &= \int_{-\infty}^{\infty} g(x) \exp(-j2\pi f_x x) dx, \end{aligned} \quad (28)$$

where  $\mathcal{F}_x[\cdot]$  denotes Fourier transformation with respect to  $x$  and where  $f_x$  is the frequency variable associated with  $x$ .

In the development to follow, it will also be necessary to perform Fourier transformation with respect to the spatial variable  $\xi$ . As such, for an arbitrary function  $p(x; \xi)$ , we define

$$\mathcal{F}_\xi[p(x; \xi)] = \int_{-\infty}^{\infty} p(x; \xi) \exp(-j2\pi\nu\xi) d\xi. \quad (29)$$

Here, as in the DOD treatment, the frequency variable  $\nu$  is assigned to  $\xi$ .

Consider again the superposition integral [Eq. (1)]. Substituting into Eq. (28) and freely interchanging integration order, we write<sup>18</sup>

$$\begin{aligned} G(f_x) &= \int_{-\infty}^{\infty} f(\xi) \mathcal{F}_x[h(x - \xi; \xi)] d\xi \\ &= \int_{-\infty}^{\infty} f(\xi) \mathcal{F}_x[h(x; \xi)] \exp(-j2\pi f_x \xi) d\xi \\ &= \mathcal{F}_\xi\{f(\xi) \mathcal{F}_x[h(x; \xi)]\}|_{\nu=f_x}. \end{aligned} \quad (30)$$

Note that we are still utilizing the line spread function notation defined in Eq. (2). An example of the transition from  $h(x - \xi; \xi)$  to  $h(x; \xi)$  is shown in Fig. 9.

Equation (30) states that we may generate the output spectrum of a space-variant system by successive Fourier transformation of the product  $f(\xi)h(x; \xi)$  with respect to  $\xi$  and  $x$  followed by evaluation along the line  $\nu = f_x$ .

The coherent processor capable of generating the output spectrum in Eq. (30) is pictured in Fig. 10. The input  $f(\xi)$  and the line spread function mask  $h(x; \xi)$  are both placed in the front focal plane of spherical lens  $L_1$ . In the back focal plane we obtain the familiar Fourier transform relationship

$$G_0(f_x, \nu) = \int_{-\infty}^{\infty} \int_{-\infty}^{\infty} [f(\xi)h(x; \xi)] \exp[-j2\pi(f_x x + \nu\xi)] dx d\xi, \quad (31)$$

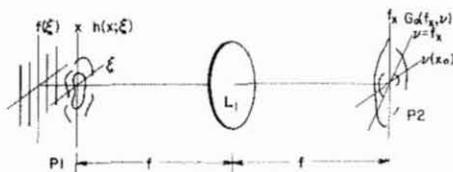


Fig. 10. A coherent optical processor for directly displaying the output spectrum of a space-variant system.



Fig. 11. When only the output intensity is of interest, the input, line spread function mask, and spherical lens may all be placed in the same plane for the OSD processor.

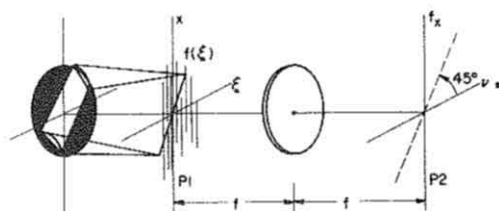


Fig. 12. The OSD processor for displaying the spectrum of a magnified input. The slope of the Dirac delta sheet on plane  $P_2$  is equal to  $M - 1$ .

where the spatial frequencies are related to the horizontal ( $x_0$ ) and vertical ( $y_0$ ) distances in the output plane by

$$f_x = y_0/\lambda f \quad \nu = x_0/\lambda f. \quad (32)$$

Note that we may write Eq. (31) as

$$G_0(f_x, \nu) = \mathcal{F}_\xi \{ f(\xi) \mathcal{F}_x [h(x; \xi)] \}. \quad (33)$$

Comparing with Eq. (30), we conclude that

$$G(f_x) = G_0(f_x, f_x). \quad (34)$$

That is, the desired 1-D output of the OSD processor in Fig. 10 lies on the  $45^\circ$  line  $\nu = f_x$  in plane  $P_2$ . Remarkably, this familiar Fourier transform configuration thus has the capability of potentially performing a wide number of space-variant operations of the form of Eq. (30).

When one is interested only in the magnitude of the output of the OSD processor, the Fourier transforming lens may be placed in the same plane as the input and line-spread function mask<sup>22</sup> (Fig. 11). One may furthermore completely discard the lens by simply including the lens's phase transmittance in the line spread function mask. In this case, we may perform 1-D space-variant processing with an input, a mask, and a few centimeters of free space. Also, note that vignetting is eliminated by such a scheme.

We now present some specific applications of the OSD processor.

#### A. Magnifier Spectrum Display

A straightforward application of the OSD processor is in displaying the spectrum of an ideal magnifier. We begin by rewriting the magnifier's line-spread function from Eq. (9) as

$$h(x; \xi) = \delta[x - (M - 1)\xi]. \quad (35)$$

As before, we may generate the required Dirac delta sheet with a cylindrical lens. The slope, however, is now equal to  $M - 1$ . The OSD processor for spectrum magnification is pictured in Fig. 12.

Experimental results displaying the spectrum of a magnified rectangular pulse are in Fig. 13. As shown, the resulting sinc functions are inversely magnified due to the scaling theorem<sup>26</sup> of Fourier transform theory. Note that, for  $M = 0$  (corresponding to a  $-45^\circ$  delta sheet input), the magnified pulse is a Dirac delta, the spectrum of which is uniform.

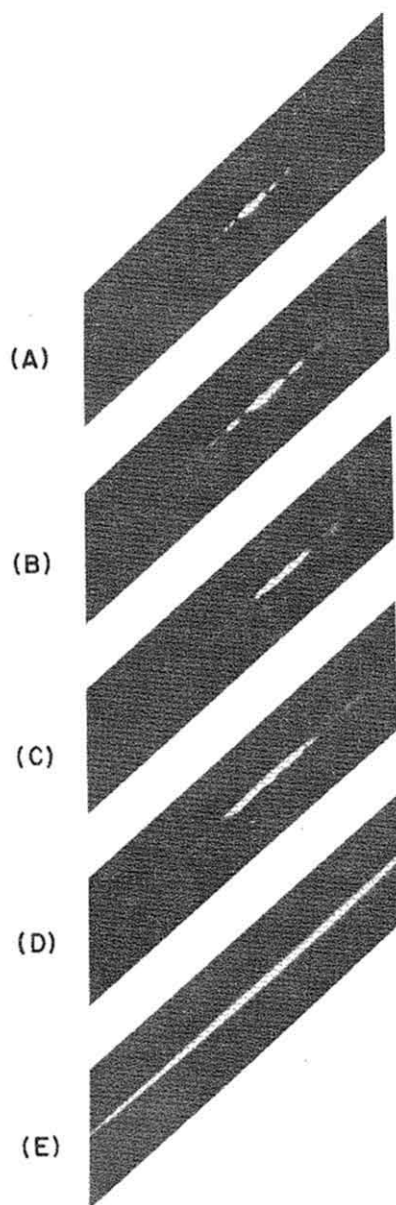


Fig. 13. The output of the OSD processor in Fig. 12 for a single square pulse input. The spectrum displays correspond to pulse magnification of (a)  $M = 2$ , (b)  $M = \frac{1}{2}$ , (c)  $M = 1$ , (d)  $M = \frac{1}{2}$ , and (e)  $M = 0$ .

## B. Cross Power Spectral Density Display

The cross power spectral density function of two signals,  $f(x)$  and  $s(x)$ , is defined as the Fourier transform of their cross-correlation:

$$S(f_x) = \int_{-\infty}^{\infty} [s(x) \star f(x)] \exp(-j2\pi f_x x) dx. \quad (36)$$

Consider, then, placing two transparencies of  $f(x)$  and  $s(x)$  in plane  $P_1$  of Fig. 10 in such a manner as to form the product  $f(x)s(x)$ . From Eq. (31), the processor output is

$$G_0(f_x, \nu) = \int_{-\infty}^{\infty} \int_{-\infty}^{\infty} f(x)s(\xi) \exp[-j2\pi(f_x x + \nu \xi)] dx d\xi. \quad (37)$$

Along the  $45^\circ$  line  $\nu = f_x$ , this becomes

$$\begin{aligned} G_0(f_x, f_x) &= \int_{-\infty}^{\infty} \int_{-\infty}^{\infty} f(x)s(\xi) \exp[-j2\pi(x + \xi)f_x] d\xi dx \\ &= \int_{-\infty}^{\infty} \int_{-\infty}^{\infty} f(x)s(\xi' - x) \exp(-j2\pi\xi' f_x) d\xi' dx, \end{aligned} \quad (38)$$

where we have made the variable substitution  $\xi' = \xi + x$ . We may rewrite Eq. (38) as

$$\begin{aligned} G_0(f_x, f_x) &= F_{\xi'}[f(\xi) \star s(\xi)] \\ &= S(f_x), \end{aligned} \quad (39)$$

which is the desired result.

## V. Generalization

We have so far restricted the input  $f(\xi)$  to be 1-D. We may easily generalize all previous schemes to utilize a 2-D input  $f(x; \xi)$ , in which case the superposition integral of Eq. (1) is augmented to the form

$$g(x) = \int_{-\infty}^{\infty} f(x; \xi) h(x - \xi; \xi) d\xi. \quad (40)$$

This relationship adds another degree of flexibility to the computational capability of the DOD and OSD processors.

## VI. Conclusions

We have presented two coherent processors capable of performing general 1-D space-variant operations. Both employ a 1-D input placed adjacent to a line spread function mask. The direct output display, or DOD processor, then performs a 1-D Fourier transform on the resulting product. The desired space-variant system output then appears along the zero frequency axis in the Fourier plane. Many recently proposed space-variant processors have been shown to be special cases of the DOD processor.

The output spectrum display, or OSD processor, directly generates the Fourier transform of the space-variant system output. Only a single spherical lens is utilized when both the output magnitude and phase are desired. No lens is required when only the output magnitude is of interest.

In practice, one may utilize a computer generated hologram for the required line spread function mask. The 1-D input can be generated by an electrical-to-optical transducer for real time applications.

The authors express their appreciation to John A. Vincent, Richard W. Thomas, Jr., and Steven V. Bell for their assistance in the preparation of this paper. This research was supported by the Air Force Office of Scientific Research, Air Force Systems Command, USAF, under grant AFOSR-75-2855A.

## References

1. O. Bryngdahl, *J. Opt. Soc. Am.* **64**, 1092 (1974).
2. W. H. Lee and O. Bryngdahl, *Opt. Commun.* **12**, 382 (1974).
3. W. T. Rhodes, "Log-frequency variable resolution optical spectrum analysis using holographic mapping techniques," to appear in *Opt. Commun.*, (1977).
4. W. T. Rhodes and J. M. Florence, *Appl. Opt.* **15**, 3073 (1976).
5. J. W. Goodman, P. Kellman, and E. W. Hansen, "Prospects for space-variant optical computing," paper presented at the 1976 International Optical Computing Conference, Capri, Italy.
6. M. R. Mueller and F. P. Carlson, *Appl. Opt.* **14**, 2207 (1975).
7. D. Casasent and D. Psaltis, "Mellin transforms in optical data processing," in *Proceedings 1975 Electro-Optical System Design Conference (Industrial and Scientific Conference Management, Inc., Chicago, 1975)*, p. 38.
8. D. Casasent and D. Psaltis, *Appl. Opt.* **15**, 1795 (1976).
9. K. Preston, *Coherent Optical Computers* (McGraw-Hill, New York, 1972).
10. D. Casasent and F. Casasayas, *Appl. Opt.* **14**, 1364 (1975).
11. R. J. Marks II, J. F. Walkup, and T. F. Krile, "Ambiguity function display: an improved coherent processor," *Appl. Opt.* **16** (April 1977).
12. A. A. Sawchuck, *J. Opt. Soc. Am.* **63**, 1052 (1973).
13. A. A. Sawchuck, *J. Opt. Soc. Am.* **64**, 138 (1974).
14. J. Duvernoy, *J. Opt. Soc. Am.* **65**, 1331 (1975).
15. L. M. Deen, J. F. Walkup, and M. O. Hagler, *Appl. Opt.* **14**, 2438 (1975).
16. J. F. Walkup and M. O. Hagler, "Volume hologram representations of space-variant optical systems," in *Proceedings 1975 Electro-Optical System Design Conference (Industrial and Scientific Conference Management Inc., Chicago, 1975)*.
17. R. J. Marks II and T. F. Krile, *Appl. Opt.* **15**, 2241 (1976).
18. R. J. Marks II, J. F. Walkup, and M. O. Hagler, *J. Opt. Soc. Am.* **66**, 918 (1976).
19. J. W. Goodman, *Proc. IEEE* **65**, (January 1977).
20. L. J. Cutrona, E. N. Leith, C. J. Palermo, and L. J. Porcello, *IRE Trans. Inf. Theory* **IT-6**, 386 (1960).
21. L. J. Cutrona, "Recent developments in coherent optical technology," in *Optical and Electro-Optical Information Processing*, J. T. Tippet *et al.*, Eds. (MIT Press, Cambridge, 1965).
22. J. W. Goodman, *Introduction to Fourier Optics* (McGraw-Hill, New York, 1968).
23. R. J. Marks II, J. F. Walkup, and M. O. Hagler, *Appl. Opt.* **15**, 2289 (1976).
24. C. M. Vest, *J. Opt. Soc. Am.* **64**, 1215 (1974).
25. J. B. Thomas, *An Introduction to Statistical Communication Theory* (Wiley, New York, 1969), p. 646.
26. R. N. Bracewell, *The Fourier Transform and its Applications* (McGraw-Hill, New York, 1965).